

Secure Transmit Antenna Selection Protocol for MIMO NOMA Networks over Nakagami- m Channels

Duc-Dung Tran, Ha-Vu Tran, Dac-Binh Ha, and Georges Kaddoum

Abstract—In this paper, we studied a multi-input multi-output (MIMO) non-orthogonal multiple access (NOMA) network consisting of one source and two legitimate users (LUs), so-called near and far users according to their distances to the source, and one passive eavesdropper, over Nakagami- m fading channel. Specifically, we investigated the scenario that the signals of the far user might or might not be decoded successfully at the eavesdropper and the near user. Thus, we aimed at designing a transmit antenna selection (TAS) secure communication protocol for the network. Then, two TAS solutions, namely Solutions I and II, were proposed. Specifically, solutions I and II focus on maximizing the received signal power between the source and the near user, and between the source and the far user, respectively. Accordingly, the exact and asymptotic closed-form expressions of the secrecy outage probability for the LUs and the overall system were derived. Our analytical results corroborated by Monte Carlo simulation indicate that the secrecy performance could be significantly improved by properly selecting power allocation coefficients and increasing the number of antennas at the source and the LUs. Interestingly, solution II could provide a better overall secrecy performance over solution I.

Index Terms—Transmit antenna selection, MIMO, non-orthogonal multiple access, physical layer security.

I. INTRODUCTION

Non-orthogonal multiple access (NOMA) has been recently considered as a promising solution for the next generation of wireless communication networks (i.e., 5G) to improve the spectral efficiency and user fairness [1]–[3]. The principle of NOMA relies on utilizing the power domain to serve multiple users at the same time/frequency/code [2]. Specifically, in a NOMA network with more than two users, a base station (BS) transmits the messages superposed with different power levels to users [4]–[6]. The power allocation is carried out based on the users' channel conditions. In principle, the successive interference cancellation (SIC) scheme is employed. First, a user detects the messages of other users with weaker channel conditions (i.e., weak users) and then removes these components from its observation. Second, it decodes its own messages by treating the messages of the other (i.e., the users with stronger channel conditions, so-called strong users) as noises. Therefore, in comparison with conventional multiple access

schemes, the NOMA can give a better user fairness because the users with weak channel conditions can be appropriately served.

With the development of wireless networks, information security is a critical challenge due to the broadcast nature of wireless transmissions [7], [8]. Recently, physical layer security (PLS) has been emerging as a prominent candidate for improving the secrecy performance of wireless systems [9]–[12]. The key idea of the PLS relies on exploiting the characteristics of wireless channels to guarantee secure communications [8]. This approach is different from traditional security solutions, such as cryptographic protocols in the upper layers [13]. In the PLS, it is well-known that the perfect secrecy is achieved when the quality of the legitimate channel is higher than that of illegitimate channel [7]–[12]. To obtain further significant improvements, many PLS-based transmission methods have been proposed, based on the applications of multi-input multi-output (MIMO) [14], [15], artificial noises [16], jamming [17], or beamforming techniques [18].

Nowadays, the approach of the PLS in NOMA systems is becoming an interesting topic [19]–[23]. In [19], the secrecy sum rate of a single-input single-output (SISO) NOMA system has been studied and the closed-form optimal solution of power allocation has been derived, based on the users' quality of service (QoS) requirements. Taking the PLS of large-scale NOMA networks into account, the work [20] has employed stochastic geometry methods to locate users and eavesdroppers in the system. Furthermore, a protected zone around the source has been introduced to enhance the information security. To characterize the secrecy performance of the proposed system, new exact and asymptotic expressions of the secrecy outage probability have been derived. In [21], the application of multiple antennas, artificial noises (AN) and a protected zone to NOMA in large-scale networks have been studied for the purpose of improving the secrecy performance. The obtained results regarding the secrecy outage probability indicated that a significant secrecy performance gain could be achieved by generating the AN at the BS and invoking the protected zone. In addition, the PLS in a two-user multi-input single-output (MISO) NOMA system was examined in [22] where NOMA is performed based on the users' QoS requirements, instead of their channel conditions. In this context, the authors considered a scenario that the eavesdropper detects two-user data using SIC. Specifically, it first treats the message of the user with a low QoS as noise to decode the message of the user with high QoS, and then subtracts this component from its observation

Duc-Dung Tran and Dac-Binh Ha are with the Faculty of Electrical & Electronics Engineering, Duy Tan University, Danang, Vietnam (e-mail: tranucdung@dtu.edu.vn, hadacbinh@duytan.edu.vn)

Ha-Vu Tran and Georges Kaddoum are with LACIME Laboratory, ETS Engineering School, University of Quebec, Montreal, Canada (e-mail: ha-vu.tran.1@ens.etsmtl.ca, georges.kaddoum@etsmtl.ca).

before decoding the message of the remaining user. Moreover, the use of a transmit antenna selection (TAS) scheme for improving secrecy performance was considered. In [23], a new secrecy beamforming (SBF) scheme for MISO NOMA systems was studied. Specifically, the proposed SBF scheme efficiently exploited AN to protect the confidential information of two NOMA assisted legitimate users (LUs). It is clear that the TAS technique has been demonstrated as a low-complexity and power-efficient solution for secure NOMA networks [22], [24].

Nevertheless, the previous works on PLS in NOMA systems [19]–[23] have not covered the following issues. First, they have considered the scenario of SISO or MISO systems with Rayleigh fading channels. Thus, the applications of MIMO which can significantly improve the secrecy performance and the consideration of Nakagami- m fading channel, which possibly bringing more insight analysis, have not been addressed yet. Second, the works [19]–[21] have been carried out under the ideal assumptions as follows: (i) the strong user always successfully decodes the message of the weak user, and (ii) the eavesdroppers have the powerful detection abilities to distinguish a multi-user data stream without the interference, generated by superposed transmit signals (i.e., worst-case eavesdropping scenario (WcES)). Unlike these studies, the authors in [22] have investigated the scenario that the eavesdropper is affected by the interference generated by superposed signals when carrying out a multi-user data detection as discussed above. However, they have assumed that the message of the user with high QoS is already decoded successfully at the eavesdropper when analyzing the secrecy performance of the user with low QoS. Meanwhile, the work [23] has considered both transmission outage¹ and secrecy outage for analyzing the secrecy performance. However, the WcES was still examined. In fact, although the WcES is an effective approach to characterize the secrecy performance, this can overestimate the eavesdropper's multi-user decodability.

Motivated by the aforementioned issues, in this paper, we proposed a new TAS-based secrecy communication protocol for two-user MIMO NOMA networks over Nakagami- m fading channels, under the following scenario. In our system model, a source transmits information, following the principle of NOMA, to two LUs², so-called near and far users. Also, a passive eavesdropper wants to extract the information from the source to LUs channels. On the transmitter side, the source broadcasts the mixed messages to the two LUs by using TAS. On the receiver side, it is assumed that maximal ratio combining (MRC) is employed at the two LUs and the eavesdropper to maximize the signal quality. Particularly, regarding the eavesdropper's multi-user decodability, we considered the cases that the eavesdropper can successfully and

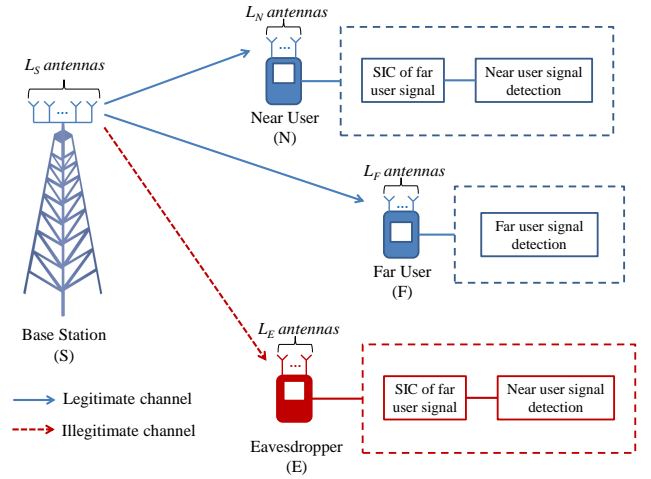


Fig. 1. System model for secure transmission in MIMO NOMA networks.

unsuccessfully decode the far user's message to analyze the secrecy performance of the near user. On this basis, two solutions of TAS to design a secure communication protocol, namely Solutions I and II, were proposed to maximize the received signal power at the near and far users, respectively. To analyze the secrecy performance of the two solutions, we derived the exact closed-form expressions of the secrecy outage probability (SOP) for the two LUs and the overall system. Also, we provided the asymptotic expressions of the SOP and investigate the secrecy diversity. Moreover, we then compared the secrecy performance in various scenarios adopting the two solutions, such as SISO versus MIMO, and compared our solutions with the previous works [21]–[23] to evaluate the benefits of our proposed protocol. Accordingly, to validate the analytical results, Monte Carlo simulation was employed.

Therefore, the contributions of this paper are summarized as follows:

- Analyzing the secrecy performance of the NOMA network in which the impact of MIMO, Nakagami- m fading, and the eavesdropper's multi-user decodability are addressed.
- Proposing two new TAS solutions to improve the security for the considered NOMA network.
- Deriving the closed-form expressions of the SOP at the LU sides and also for the overall network to evaluate the secrecy performance of our solutions.
- Providing the asymptotic expressions of the SOPs and investigating the secrecy diversity order.

The remainder of the paper is organized as follows: The system model is presented in Section II. The transmit antenna selection scheme is described in Section III. The secrecy performance analysis of the considered system is shown in Section IV. The numerical results and discussions are depicted in Section V. Finally, Section VI shows our conclusion.

¹In a two-user NOMA system, the transmission outage occurs at the strong user when it does not successfully decode the message of the weak user or its own message.

²In order to focus on designing a new secrecy communication protocol, a two-user NOMA network is studied in this paper. In particular, our obtained results can be easily used for further calculations in downlink NOMA systems with multiple users (more than two users) by applying the hybrid multiple access techniques (i.e., the combination between NOMA and conventional OMA schemes) as studied in [25], [26].

II. SYSTEM MODEL

Consider a downlink MIMO NOMA network consisting of a source (the base station) denoted by S , a near user denoted by N , a far (cell edge) user denoted by F , and a passive eavesdropper denoted by E , as depicted in Fig. 1. In this system, the source S , the near user N , the far user F , and the eavesdropper E are equipped with L_S , L_N , L_F , and L_E antennas, respectively.

Let $h_{U_j S_i}$ ($1 \leq i \leq L_S$, $1 \leq j \leq L_U$, $U \in \{N, F\}$) denotes the channel fading coefficient from antenna i at S to antenna j at U . Similarly, $h_{E_j S_i}$ ($1 \leq j \leq L_E$) denotes the channel fading coefficient from antenna i at source S to antenna j at E . In our work, legitimate and eavesdropping channels are modeled as mutually independent and identically distributed (i.i.d) Nakagami- m fading ones with parameters m_U and m_E , and squared means $\Omega_U = \mathbb{E} \left[|h_{U_j S_i}|^2 \right]$ and $\Omega_E = \mathbb{E} \left[|h_{E_j S_i}|^2 \right]$, respectively. In addition, the distance and path loss exponent of $S \rightarrow U$ and $S \rightarrow E$ channels are denoted by d_{US} and θ_{US} , and d_{ES} and θ_{ES} , respectively.

Employing the NOMA technique, S simultaneously communicates with two LUs N and F . Further, S selects an antenna among L_S antennas to broadcast information to N and F by applying a TAS technique. The antenna selection schemes will be clarified in the next section. At the receiver side, maximal ratio combining (MRC) is used at N , F , and E .

Suppose that antenna i at S is selected for transmission, the channel gain of $S \rightarrow U$ link can be expressed as

$$\|\mathbf{h}_{US_i}\|^2 = \sum_{j=1}^{L_U} |h_{U_j S_i}|^2, \quad (1)$$

where $\mathbf{h}_{US_i} \in \mathbb{C}^{L_U \times 1}$ denotes the channel coefficient vector of $S \rightarrow U$ link.

Given the above discussion, the overall communication process of the system can be mathematically depicted as follows. Following the principle of NOMA, S transmits the superposed message $x = \sqrt{\alpha_N P_S} x_N + \sqrt{\alpha_F P_S} x_F$ to N and F , where x_N and x_F denote the intended messages for N and F , respectively. Also α_N and α_F denote power allocation coefficient for N and F , respectively. Thus, the received signal at U ($U \in \{N, F\}$) is given by

$$y_{US_i} = \left(\sqrt{\alpha_N P_S} x_N + \sqrt{\alpha_F P_S} x_F \right) \mathbf{w}_{US_i} \mathbf{h}_{US_i} + n_{US_i}, \quad (2)$$

where $\mathbf{w}_{US_i} = \frac{\mathbf{h}_{US_i}^\dagger}{\|\mathbf{h}_{US_i}\|}$ represents the signal processing operation at U with MRC, $n_{US_i} \sim \mathcal{CN}(0, N_0)$ stands for an additive white Gaussian noise (AWGN) at user U . According to the principle of NOMA, we assume that $\|\mathbf{h}_{NS_i}\|^2 > \|\mathbf{h}_{FS_i}\|^2$, $\alpha_F > \alpha_N > 0$ and $\alpha_F + \alpha_N = 1$. Therefore, the instantaneous signal-to-interference-and-noise ratio (SINR) at F to detect x_F is

$$\gamma_{FS_i}^{x_F} = \frac{\alpha_F \gamma_0 \|\mathbf{h}_{FS_i}\|^2}{\alpha_N \gamma_0 \|\mathbf{h}_{FS_i}\|^2 + 1}, \quad (3)$$

where $\gamma_0 = \frac{P_S}{N_0}$ denotes the average transmit signal-to-noise ratio (SNR) associated with the LUs.

At N , a SIC receiver is used to decode x_F which is then removed from the observation before detecting x_N . Thus, the instantaneous SINR at N to detect x_F can be given by

$$\gamma_{NS_i}^{x_F} = \frac{\alpha_F \gamma_0 \|\mathbf{h}_{NS_i}\|^2}{\alpha_N \gamma_0 \|\mathbf{h}_{NS_i}\|^2 + 1}, \quad (4)$$

and the instantaneous SNR at N to detect x_N is written as

$$\gamma_{NS_i}^{x_N} = \alpha_N \gamma_0 \|\mathbf{h}_{NS_i}\|^2. \quad (5)$$

At E , the signal received from S can be expressed as

$$y_{ES_i} = \left(\sqrt{\alpha_N P_S} x_N + \sqrt{\alpha_F P_S} x_F \right) \mathbf{w}_{ES_i} \mathbf{h}_{ES_i} + n_{ES_i}, \quad (6)$$

where $\mathbf{w}_{ES_i} = \frac{\mathbf{h}_{ES_i}^\dagger}{\|\mathbf{h}_{ES_i}\|}$ represents the signal processing operation at E with MRC, $n_{ES_i} \sim \mathcal{CN}(0, N_E)$ stands for the AWGN at E . We assume that SIC receiver is applied at E to decode x_F , then subtract this element from the received signal to detect x_N . Thus, the instantaneous SINR at E to detect x_F can be expressed as

$$\gamma_{ES_i}^{x_F} = \frac{\alpha_F \gamma_E \|\mathbf{h}_{ES_i}\|^2}{\alpha_N \gamma_E \|\mathbf{h}_{ES_i}\|^2 + 1}, \quad (7)$$

and the instantaneous SNR at E to detect x_N is written as

$$\gamma_{ES_i}^{x_N} = \alpha_N \gamma_E \|\mathbf{h}_{ES_i}\|^2, \quad (8)$$

where $\gamma_E = \frac{P_S}{N_E}$ is the average transmit SNR associated with E .

III. PROPOSED TAS PROTOCOL AND PRELIMINARIES

In this section, we propose two solutions, namely Solutions I and II, for designing a TAS-based secure protocol for the MIMO NOMA network.

A. Two Proposed TAS Solutions

For convenience, let $X_i = \|\mathbf{h}_{FS_i}\|^2$, $Y_i = \|\mathbf{h}_{NS_i}\|^2$, and $Z_i = \|\mathbf{h}_{ES_i}\|^2$.

1) *Solution I and Formulations of Legitimate Channels:* In solution I, an antenna at S is selected for transmission with the aim of finding the best channel condition of $S \rightarrow N$ link.

Given this context, the selected antenna, denoted by \hat{i} , can be mathematically represented as follows:

$$\hat{i} = \arg \max_{1 \leq i \leq L_S} \{Y_i\}. \quad (9)$$

With this setting, the CDF of $Y_{\hat{i}}$ has the following form [14]

$$F_{Y_{\hat{i}}, I}(x) = \left(1 - \sum_{k=0}^{a_N-1} \frac{m_N^k}{k! \lambda_{NS}^k} x^k e^{-\frac{m_N x}{\lambda_{NS}}} \right)^{L_S}, \quad (10)$$

where $a_N = m_N L_N$ and $\lambda_{NS} = \frac{\Omega_N}{d_{NS}^{\theta_{NS}}}$.

With the aid of the binomial expansion given in [27, Eq. 1.111] and using the multinomial theorem, (10) can be rewritten as

$$F_{Y_{\hat{i}}, I}(x) = 1 + \sum_{p=1}^{L_S} \sum_{\Delta_N=p} \Phi_N x^{\varphi_N} e^{-\frac{p m_N x}{\lambda_{NS}}}, \quad (11)$$

where $\Delta_N = \sum_{q=0}^{a_N-1} \delta_{N,q}$, $\varphi_N = \sum_{q=0}^{a_N-1} q\delta_{N,q}$, and $\Phi_N = \binom{L_S}{p} (-1)^p \binom{p}{\delta_{N,0}, \dots, \delta_{N,a_N-1}} \left[\prod_{q=0}^{a_N-1} \left(\frac{m_N^q}{q! \lambda_{NS}^q} \right)^{\delta_{N,q}} \right]$.

For F , the CDF of X_i is given by [14]

$$F_{X_i, I}(x) = 1 - \sum_{k=0}^{a_F-1} \frac{m_F^k}{k! \lambda_{FS}^k} x^k e^{-\frac{m_F x}{\lambda_{FS}}}, \quad (12)$$

where $a_F = m_F L_F$ and $\lambda_{FS} = \frac{\Omega_F}{d_{FS}^{\theta_{FS}}}$.

2) *Solution II and Formulations of Legitimate Channels:*

Different from Solution I, in Solution II, an antenna at S is chosen to broadcast information with the purpose of providing the best channel gain of $S \rightarrow F$ link. Accordingly, the chosen antenna at S in this case can be expressed as

$$\hat{i} = \arg \max_{1 \leq i \leq L_S} \{X_i\}. \quad (13)$$

Thus, the CDF of X_i can be given as

$$F_{X_i, II}(x) = 1 + \sum_{p=1}^{L_S} \sum_{\Delta_F=p} \Phi_F x^{\varphi_F} e^{-\frac{p m_F x}{\lambda_{FS}}}, \quad (14)$$

and the CDF of Y_i is

$$F_{Y_i, II}(x) = 1 - \sum_{k=0}^{a_N-1} \frac{m_N^k}{k! \lambda_{NS}^k} x^k e^{-\frac{m_N x}{\lambda_{NS}}}, \quad (15)$$

where $\Delta_F = \sum_{q=0}^{a_F-1} \delta_{F,q}$, $\varphi_F = \sum_{q=0}^{a_F-1} q\delta_{F,q}$, and $\Phi_F = \binom{L_S}{p} (-1)^p \binom{p}{\delta_{F,0}, \dots, \delta_{F,a_F-1}} \left[\prod_{q=0}^{a_F-1} \left(\frac{m_F^q}{q! \lambda_{FS}^q} \right)^{\delta_{F,q}} \right]$.

3) *Formulations of Eavesdropping Channels:* For E , the PDF and the CDF of Z_i in both Solutions I and II are given by [14]

$$f_{Z_i}(x) = \frac{m_E^{a_E} x^{a_E-1}}{\Gamma(a_E) \lambda_{ES}^{a_E}} e^{-\frac{m_E x}{\lambda_{ES}}}, \quad (16)$$

$$F_{Z_i}(x) = 1 - \sum_{k=0}^{a_E-1} \frac{m_E^k}{k! \lambda_{ES}^k} x^k e^{-\frac{m_E x}{\lambda_{ES}}}, \quad (17)$$

where $a_E = m_E L_E$ and $\lambda_{ES} = \frac{\Omega_E}{d_{ES}^{\theta_{ES}}}$.

B. Preliminary Analysis of SINRs with Solutions I and II

From (12), (14), and (17), the closed-form expressions of the CDF of $\gamma_{FS_i}^{x_F}$ in Solutions I and II, and the PDF of $\gamma_{ES_i}^{x_F}$ are calculated through Lemma 1, Lemma 2, and Lemma 3, respectively, as follows.

Lemma 1. *Under Nakagami- m fading, the CDF of $\gamma_{FS_i}^{x_F}$ in Solution I has the following form*

$$F_{\gamma_{FS_i}^{x_F}, I}(x) = \begin{cases} 1, & x \geq \beta \\ 1 - \sum_{k=0}^{a_F-1} \frac{1}{k! \lambda_{FS}^k} \left(\frac{m_F A_x}{\gamma_0} \right)^k e^{-\frac{m_F A_x}{\gamma_0}}, & x < \beta \end{cases}, \quad (18)$$

where $A_x = \frac{x}{\alpha_F - \alpha_N x}$ and $\beta = \frac{\alpha_F}{\alpha_N}$.

Proof: With the aid of (3), $F_{\gamma_{FS_i}^{x_F}, I}(x)$ is given by

$$F_{\gamma_{FS_i}^{x_F}, I}(x) = \Pr \left(\frac{\alpha_F \gamma_0 X_i}{\alpha_N \gamma_0 X_i + 1} < x \right) = \begin{cases} 1, & x \geq \beta \\ \Pr \left(X_i < \frac{A_x}{\gamma_0} \right), & x < \beta \end{cases} \quad (19)$$

$$= \begin{cases} 1, & x \geq \beta \\ F_{X_i, I} \left(\frac{A_x}{\gamma_0} \right), & x < \beta \end{cases}.$$

By substituting (12) into (19), (18) is obtained and the proof is completed. ■

Lemma 2. *Under Nakagami- m fading, the CDF of $\gamma_{FS_i}^{x_F}$ in Solution II is expressed as*

$$F_{\gamma_{FS_i}^{x_F}, II}(x) = \begin{cases} 1, & x \geq \beta \\ 1 + \sum_{p=1}^{L_S} \sum_{\Delta_F=p} \Phi_F \left(\frac{A_x}{\gamma_0} \right)^{\varphi_F} e^{-\frac{p m_F A_x}{\gamma_0 \lambda_{FS}}}, & x < \beta \end{cases}. \quad (20)$$

Proof: Similar to the proof of Lemma 1, based on (3), $F_{\gamma_{FS_i}^{x_F}, II}(x)$ can be represented as

$$F_{\gamma_{FS_i}^{x_F}, II}(x) = \begin{cases} 1, & x \geq \beta \\ F_{X_i, II} \left(\frac{A_x}{\gamma_0} \right), & x < \beta \end{cases}. \quad (21)$$

To this end, by substituting (14) into (21) to obtain (20), the proof is completed. ■

Lemma 3. *Under Nakagami- m fading, the PDF of $\gamma_{ES_i}^{x_F}$ is given by*

$$f_{\gamma_{ES_i}^{x_F}}(x) = \begin{cases} 0, & x \geq \beta \\ \sum_{k=0}^{a_E-1} \frac{m_E^k \alpha_F A_x^{k-1} e^{-\frac{m_E A_x}{\gamma_E \lambda_{ES}}}}{k! \lambda_{ES}^k \gamma_E^k (\alpha_F - \alpha_N x)^2} \left(\frac{m_E A_x}{\lambda_{ES} \gamma_E} - k \right), & x < \beta \end{cases}. \quad (22)$$

Proof: First, we derive the CDF of $\gamma_{ES_i}^{x_F}$ by using (7) as follows:

$$F_{\gamma_{ES_i}^{x_F}}(x) = \begin{cases} 1, & x \geq \beta \\ F_{Z_i} \left(\frac{A_x}{\gamma_E} \right), & x < \beta \end{cases}. \quad (23)$$

By substituting (17) into (23), $F_{\gamma_{ES_i}^{x_F}}(x)$ is expressed as

$$F_{\gamma_{ES_i}^{x_F}}(x) = \begin{cases} 1, & x \geq \beta \\ 1 - \sum_{k=0}^{a_E-1} \frac{1}{k! \lambda_{ES}^k} \left(\frac{m_E A_x}{\gamma_E} \right)^k e^{-\frac{m_E A_x}{\gamma_E \lambda_{ES}}}, & x < \beta \end{cases}. \quad (24)$$

The PDF of $\gamma_{ES_i}^{x_F}$ is defined as

$$f_{\gamma_{ES_i}^{x_F}}(x) = \frac{dF_{\gamma_{ES_i}^{x_F}}(x)}{dx}. \quad (25)$$

The final expression of $f_{\gamma_{ES_i}^{x_F}}(x)$ in (22) is obtained by deriving the derivative of $F_{\gamma_{ES_i}^{x_F}}(x)$ in (24) with respect to x . The proof is completed. ■

IV. SECRECY PERFORMANCE ANALYSIS

In this section, to validate the two proposed solutions, the secrecy performance regarding the SOP obtained at N and F , and the SOP of the overall system is analyzed.

A. Preliminary

This subsection presents the definitions of secrecy capacity and SOP for secure communication in the considered MIMO NOMA system.

First, let $C_{U,i}$ and $C_{EU,i}$ ($U \in \{N, F\}$) denote the capacities of $S \rightarrow U$ legitimate channel and $S \rightarrow E$ illegitimate channel to detect the signal x_U , respectively. Thus, according to [9], the secrecy capacity achieved at U can be defined as

$$\begin{aligned} C_{S,i} &= \max\{0, C_{U,i} - C_{EU,i}\} \\ &= \max\left\{0, \log_2\left(\frac{1 + \gamma_{US_i}^{x_U}}{1 + \gamma_{ES_i}^{x_U}}\right)\right\}, \end{aligned} \quad (26)$$

where $C_{U,i} = \log_2(1 + \gamma_{US_i}^{x_U})$ and $C_{EU,i} = \log_2(1 + \gamma_{ES_i}^{x_U})$.

Second, the SOP obtained at N is defined as

$$\begin{aligned} SOP_{N,i} &= \Pr\{\gamma_{NS_i}^{x_F} < \gamma_F\} \\ &+ \Pr\{\gamma_{NS_i}^{x_F} \geq \gamma_F, \gamma_{ES_i}^{x_F} < \gamma_F, C_{N,i} < R_{s,N}\} \\ &+ \Pr\{\gamma_{NS_i}^{x_F} \geq \gamma_F, \gamma_{ES_i}^{x_F} \geq \gamma_F, C_{S,i} < R_{s,N}\}, \end{aligned} \quad (27)$$

where $\gamma_F = 2^{R_F} - 1$ denotes the SNR threshold for correctly decoding x_F , R_F represents the target data rate of F , and $R_{s,N}$ represents the secrecy rate threshold at N .

Remark 1. Particularly, the definition of $SOP_{N,i}$, given in (27), is different from the previous works considering the scenario that N and E are always decode successfully the message of F , i.e., $\Pr\{\gamma_{NS_i}^{x_F} \geq \gamma_F\} = 1$ [19]–[22] and $\Pr\{\gamma_{ES_i}^{x_F} \geq \gamma_F\} = 1$ [19]–[23].

To analyze the SOP at user N , its formulation needs to be further expressed for more insights. Thus, according to (27), $SOP_{N,i}$ can be expressed as in Lemma 4.

Lemma 4. The SOP at user N can be given as

$$\begin{aligned} SOP_{N,i} &= \underbrace{\Pr\{\gamma_{NS_i}^{x_F} < \gamma_F\}}_{\Theta_1} \\ &+ \underbrace{\Pr\{\gamma_{NS_i}^{x_F} \geq \gamma_F, \gamma_{ES_i}^{x_F} < \gamma_F, C_{N,i} < R_{s,N}\}}_{\Theta_2} \\ &+ \underbrace{\Pr\{\gamma_{NS_i}^{x_F} \geq \gamma_F, \gamma_{ES_i}^{x_F} \geq \gamma_F, C_{S,i} < R_{s,N}\}}_{\Theta_3} \\ &= \begin{cases} 1, & \gamma_F \geq \beta \\ \Lambda_1 + \Lambda_2 + \Lambda_3, & \gamma_F < \beta \end{cases}, \end{aligned} \quad (28)$$

where Λ_1 , Λ_2 , and Λ_3 are, respectively, given by

$$\begin{aligned} \Lambda_1 &= F_{Y_i}\left(\frac{A_{\gamma_F}}{\gamma_0}\right), \\ \Lambda_2 &= \begin{cases} 0, & R_{s,N} < \eta \\ \left[F_{Y_i}\left(\frac{\gamma_{s,N}}{\gamma_0}\right) - F_{Y_i}\left(\frac{A_{\gamma_F}}{\gamma_0}\right) \right] \\ \times F_{Z_i}\left(\frac{A_{\gamma_F}}{\gamma_E}\right), & R_{s,N} > \eta \end{cases}, \end{aligned}$$

and

$$\Lambda_3 = \int_{\frac{A_{\gamma_F}}{\gamma_E}}^{\infty} \left[F_{Y_i}\left(\frac{2^{R_{s,N}} \gamma_E x + \gamma_{s,N}}{\gamma_0}\right) - F_{Y_i}\left(\frac{A_{\gamma_F}}{\gamma_0}\right) \right] f_{Z_i}(x) dx,$$

where $\eta = \log_2\left(\frac{\alpha_F}{\alpha_F - \alpha_N \gamma_F}\right)$ and $\gamma_{s,N} = \frac{2^{R_{s,N}} - 1}{\alpha_N}$.

Proof: See Appendix A. ■

Third, the SOP at F has the following form

$$\begin{aligned} SOP_{F,i} &= \Pr\{C_{F,i} - C_{EF,i} < R_{s,F}\} \\ &= \int_0^{\infty} F_{\gamma_{FS_i}^{x_F}}(g_{x,F}) f_{\gamma_{ES_i}^{x_F}}(x) dx, \end{aligned} \quad (29)$$

where $g_{x,F} = 2^{R_{s,F}} x + 2^{R_{s,F}} - 1$ and $R_{s,F}$ represents the secrecy rate threshold at F .

Fourth, in the system, we define the overall SOP as the probability that the secrecy outage event occurs at either N or F , i.e.,

$$SOP_{O,i} = 1 - (1 - SOP_{F,i})(1 - SOP_{N,i}). \quad (30)$$

B. Secrecy Performance Analysis of Solution I

1) *Exact Secrecy Outage Probability Analysis:* In this case, the SOP at F and N are derived through Theorem 1 and Theorem 2 as follows.

Theorem 1. Under Nakagami- m fading, the SOP of user F in Solution I is approximately expressed as

$$SOP_{F,I} \approx 1 - \sum_{m=0}^{a_F} \sum_{n=0}^{a_E} \sum_{i=0}^N \Psi_{F,I}^{(1)} h_{F,I} \left[\frac{(v_i + 1) u_F}{2} \right], \quad (31)$$

where $\Psi_{F,I}^{(1)} = \frac{\pi u_F \alpha_F m_F^m m_E^n \sqrt{1 - v_i^2}}{m! n! 2N \lambda_{FS}^m \lambda_{ES}^n \gamma_0^m \gamma_n^n}$, $v_i = \cos\left[\frac{(2i-1)\pi}{2N}\right]$, $u_F = \frac{1}{\alpha_N 2^{R_{s,F}}} - 1$, $h_{F,I}(x) = \frac{A_{g_{x,F}}^{m_F} A_x^{n-1}}{(\alpha_F - \alpha_N x)^2} e^{-\frac{m_F A_{g_{x,F}}}{\gamma_0 \lambda_{FS}} - \frac{m_E A_x}{\gamma_E \lambda_{ES}}} \left(\frac{m_E A_x}{\gamma_E \lambda_{ES}} - n\right)$, $g_{x,F} = 2^{R_{s,F}} x + 2^{R_{s,F}} - 1$, and N is a complexity-accuracy trade-off parameter.

Proof: See Appendix B. ■

Theorem 2. Under Nakagami- m fading, the SOP of user N in Solution I is given by

$$SOP_{N,I} = \begin{cases} 1, & \gamma_F \geq \beta \\ \Lambda_{1,I} + \Lambda_{2,I} + \Lambda_{3,I}, & \gamma_F < \beta \end{cases}, \quad (32)$$

where

$$\begin{aligned} \Lambda_{1,I} &= F_{Y_i,I}\left(\frac{A_{\gamma_F}}{\gamma_0}\right), \\ \Lambda_{2,I} &= \begin{cases} 0, & R_{s,N} < \eta \\ \left[F_{Y_i,I}\left(\frac{\gamma_{s,N}}{\gamma_0}\right) - F_{Y_i,I}\left(\frac{A_{\gamma_F}}{\gamma_0}\right) \right] \\ \times F_{Z_i}\left(\frac{A_{\gamma_F}}{\gamma_E}\right), & R_{s,N} > \eta \end{cases}, \\ \Lambda_{3,I} &= B_{N,I}^{(1)} + \sum_{p, \Delta_N, m, n} \Psi_{N,I} \left[\frac{A_{\gamma_F} B_{N,I}^{(2)}}{\gamma_E} \right]^n e^{-\frac{A_{\gamma_F} B_{N,I}^{(2)}}{\gamma_E}}, \end{aligned}$$

with $F_{Y_{\hat{i},I}}(x)$ and $F_{Z_{\hat{i}}}(x)$ are defined in (11) and (17), respectively. $B_{N,I}^{(1)} = \left[1 - F_{Y_{\hat{i},I}}\left(\frac{A_{\gamma_F}}{\gamma_0}\right)\right] \left[1 - F_{Z_{\hat{i}}}\left(\frac{A_{\gamma_F}}{\gamma_E}\right)\right]$, $B_{N,I}^{(2)} = \frac{pm_N \gamma_E 2^{R_{s,N}}}{\gamma_0 \lambda_{NS}} + \frac{m_E}{\lambda_{ES}}$, $\sum_{p,\Delta_N,m,n} = \sum_{p=1}^{L_S} \sum_{\Delta_N=p} \sum_{m=0}^{\varphi_N} \sum_{n=0}^{a_E+m-1}$, and $\Psi_{N,I} = \left(\frac{\varphi_N}{m}\right) \frac{\Phi_N \Gamma(a_E+m) m_E^{a_E} (2^{R_{s,N}} \gamma_E)^m \gamma_{s,N}^{\varphi_N-m} e^{-\frac{pm_N \gamma_{s,N}}{\gamma_0 \lambda_{NS}}}}{n! \Gamma(a_E) \lambda_{ES}^m \gamma_0^{\varphi_N} [B_{N,I}^{(2)}]^{a_E+m}}$.

Proof: See Appendix C. ■

From (30), the overall SOP of the system in Solution I is expressed as

$$SOP_{O,I} = 1 - (1 - SOP_{F,I})(1 - SOP_{N,I}). \quad (33)$$

2) *Asymptotic Secrecy Outage Probability Analysis*: Using the series representation of e^x given by [27, Eq. 1.211]

$$e^x = \sum_{k=0}^{\infty} \frac{x^k}{k!}, \quad (34)$$

the asymptotic CDF of $X_{\hat{i}}$ and $Y_{\hat{i}}$ when $\gamma_0 \rightarrow \infty$ are written as

$$F_{X_{\hat{i},I}}(x) \approx \frac{(m_F x / \lambda_{FS})^{a_F}}{(a_F)!}, \quad (35)$$

and

$$F_{Y_{\hat{i},I}}(x) \approx \left[\frac{(m_N x / \lambda_{NS})^{a_N}}{(a_N)!} \right]^{L_S}, \quad (36)$$

respectively.

For F , according to Lemma 1, (29), and (35), after some algebraic manipulations similar to the proof of Theorem 1 in Appendix B, its SOP in Solution I is asymptotically approximated as

$$SOP_{F,I}^{asym} \approx \sum_{m=0}^{a_E-1} \sum_{i=0}^N \Psi_{F,I}^{asym} h_{F,I}^{asym} \left[\frac{(v_i + 1) u_F}{2} \right] + \sum_{m=0}^{a_E-1} \Psi_{F,E}, \quad (37)$$

where $\Psi_{F,E} = \frac{m_E^m A_{u_F} e^{-\frac{m_E A_{u_F}}{\gamma_E \lambda_{ES}}}}{m! \gamma_E^m \lambda_{ES}^m}$, $\Psi_{F,I}^{asym} = \frac{\pi u_F \alpha_F m_F^{a_F} m_E^m \sqrt{1-v_i^2}}{m! (a_F)! 2N \lambda_{FS}^{\alpha_F} \lambda_{ES}^m \gamma_0^{\alpha_F} \gamma_E^m}$, and $h_{F,I}^{asym}(x) = \frac{A_{g_{x,F}}^{a_F} A_x^{m-1} e^{-\frac{m_E A_x}{\gamma_E \lambda_{ES}}}}{(\alpha_F - \alpha_N x)^2} \left(\frac{m_E A_x}{\gamma_E \lambda_{ES}} - m \right)$.

The secrecy diversity order at F in Solution I, $D_{F,I}$, is defined as

$$D_{F,I} = - \lim_{\gamma_0 \rightarrow \infty} \frac{\log [SOP_{F,I}^{asym}(\gamma_0)]}{\log(\gamma_0)}. \quad (38)$$

By substituting (37) into (38), we have $D_{F,I} = 0$.

For N , based on (28) and (36), and after some algebraic manipulations similar to the proof of Theorem 2 in Appendix C, its asymptotic SOP in Solution I is expressed as

$$SOP_{N,I}^{asym} = \begin{cases} 1, & \gamma_F \geq \beta \\ \Lambda_{1,I}^{asym} + \Lambda_{2,I}^{asym} + \Lambda_{3,I}^{asym}, & \gamma_F < \beta \end{cases}, \quad (39)$$

where

$$\Lambda_{1,I}^{asym} \approx \frac{1}{[(a_N)!]^{L_S}} \left(\frac{m_N A_{\gamma_F}}{\gamma_0 \lambda_{NS}} \right)^{b_N},$$

$$\Lambda_{2,I}^{asym} \approx \begin{cases} 0, & R_{s,N} < \eta \\ \frac{(m_N / \gamma_0 \lambda_{NS})^{b_N}}{[(a_N)!]^{L_S}} (\gamma_{s,N}^{b_N} - A_{\gamma_F}^{b_N}) \times F_{Z_{\hat{i}}}\left(\frac{A_{\gamma_F}}{\gamma_E}\right), & R_{s,N} > \eta \end{cases},$$

$$\Lambda_{3,I}^{asym} \approx B_{N,I}^{asym} + \sum_{m=0}^{b_N} \sum_{n=0}^{a_E+m-1} \Psi_{N,I}^{asym} \left(\frac{m_E A_{\gamma_F}}{\gamma_E \lambda_{ES}} \right)^n e^{-\frac{m_E A_{\gamma_F}}{\gamma_E \lambda_{ES}}},$$

with $B_{N,I}^{asym} = \frac{(m_N A_{\gamma_F} / \gamma_0 \lambda_{NS})^{b_N}}{[(a_N)!]^{L_S}} \left[F_{Z_{\hat{i}}}\left(\frac{A_{\gamma_F}}{\gamma_E}\right) - 1 \right]$,

$\Psi_{N,I}^{asym} = \binom{b_N}{m} \frac{m_N^{b_N} \Gamma(a_E+m) \gamma_{s,N}^{b_N-m} (2^{R_{s,N}} \gamma_E)^m \lambda_{ES}^m}{n! \Gamma(a_E) [(a_N)!]^{L_S} (\gamma_0 \lambda_{NS})^{b_N} m_E^m}$, and $b_N = a_N L_S$.

The secrecy diversity order at N in Solution I, $D_{N,I}$, is given by

$$D_{N,I} = - \lim_{\gamma_0 \rightarrow \infty} \frac{\log [SOP_{N,I}^{asym}(\gamma_0)]}{\log(\gamma_0)} = \begin{cases} 0, & \gamma_F \geq \beta \\ b_N, & \gamma_F < \beta \end{cases}. \quad (40)$$

Based on (30), the overall SOP in Solution I is asymptotically derived as

$$SOP_{O,I}^{asym} = 1 - \left(1 - SOP_{F,I}^{asym}\right) \left(1 - SOP_{N,I}^{asym}\right), \quad (41)$$

and the achieved overall secrecy diversity order is

$$D_{O,I} = - \lim_{\gamma_0 \rightarrow \infty} \frac{\log [SOP_{O,I}^{asym}(\gamma_0)]}{\log(\gamma_0)} = 0. \quad (42)$$

From the asymptotic results, we provide some useful insights through the following remarks.

Remark 2. In case of $\gamma_F < \beta$, the secrecy diversity order of N is $m_N L_S L_N$. This reveals that Solution I can offer the full secrecy diversity order for N . Moreover, the increases in m_N , L_S , and L_N can help to improve the secrecy performance of N . In another case of $\gamma_F \geq \beta$, the zero secrecy diversity order for N is obtained and hence its secrecy performance is saturated as $\gamma_0 \rightarrow \infty$.

Remark 3. The secrecy diversity order is 0 for both F and the overall system in solution I. In the other words, the secrecy performance is unchanged in both the two cases (i.e., user F and the overall system) when $\gamma_0 \rightarrow \infty$. This will be further clarified in section V.

C. Secrecy Performance Analysis of Solution II

1) *Exact Secrecy Outage Probability Analysis*: In this case, the SOP at F and N are derived through Theorems 3 and 4 as follows.

Theorem 3. Under Nakagami- m fading, the SOP of F with Solution II is approximately expressed as

$$SOP_{F,II} \approx 1 + \sum_{p,\Delta_F,m,i} \Psi_{F,II}^{(1)} h_{F,II} \left[\frac{(v_i + 1) u_F}{2} \right], \quad (43)$$

$$\text{where } \sum_{p, \Delta_F, m, i}^{\sim} = \sum_{p=1}^{L_S} \sum_{\Delta_F=p} \sum_{m=0}^{a_E} \sum_{i=0}^N,$$

$$\Psi_{F,II}^{(1)} = \frac{\pi u_F \Phi_F \alpha_F m_E^m \sqrt{1-v_i^2}}{m! 2N \gamma_0^{\varphi_F} \gamma_E^m \lambda_{ES}^m}, \quad \text{and } h_{F,II}(x) = \frac{A_{g_{x,F}}^{\varphi_F} A_x^{m-1}}{(\alpha_F - \alpha_N x)^2} e^{-\frac{p m_F A_{g_{x,F}}}{\gamma_0 \lambda_{FS}} - \frac{m_E A_x}{\gamma_E \lambda_{ES}}} \left(\frac{m_E A_x}{\gamma_E \lambda_{ES}} - m \right).$$

Proof: The proof of this theorem is similar to the proof of Theorem 1 in Appendix B, in which Lemma 2 is used instead of Lemma 1. ■

Theorem 4. *Under Nakagami- m fading, the SOP of N in the case of Solution II is given by*

$$SOP_{N,II} = \begin{cases} 1, & \gamma_F \geq \beta \\ \Lambda_{1,II} + \Lambda_{2,II} + \Lambda_{3,II}, & \gamma_F < \beta \end{cases}, \quad (44)$$

where

$$\Lambda_{1,II} = F_{Y_{i,II}} \left(\frac{A_{\gamma_F}}{\gamma_0} \right),$$

$$\Lambda_{2,II} = \begin{cases} 0, & R_{s,N} < \eta \\ \left[F_{Y_{i,II}} \left(\frac{\gamma_{s,N}}{\gamma_0} \right) - F_{Y_{i,II}} \left(\frac{A_{\gamma_F}}{\gamma_0} \right) \right] \times F_{Z_i} \left(\frac{A_{\gamma_E}}{\gamma_E} \right), & R_{s,N} > \eta \end{cases},$$

and

$$\Lambda_{3,II} = B_{N,II}^{(1)} - \sum_{m,n,p}^{\sim} \Psi_{N,II} \left[\frac{A_{\gamma_F} B_{N,II}^{(2)}}{\gamma_E} \right]^n e^{-\frac{A_{\gamma_F} B_{N,II}^{(2)}}{\gamma_E}},$$

$$\text{with } B_{N,II}^{(1)} = \left[1 - F_{Y_{i,II}} \left(\frac{A_{\gamma_F}}{\gamma_0} \right) \right] \left[1 - F_{Z_i} \left(\frac{A_{\gamma_F}}{\gamma_E} \right) \right],$$

$$B_{N,II}^{(2)} = \frac{m_E}{\lambda_{ES}} + \frac{m_N \gamma_E 2^{R_{s,N}}}{\gamma_0 \lambda_{NS}}, \quad \sum_{m,n,p}^{\sim} = \sum_{m=0}^{a_N-1} \sum_{n=0}^m \sum_{p=0}^{a_E+n-1},$$

$$F_{Y_{i,II}}(x) \text{ is defined in (15), and } \Psi_{N,II} = \binom{m}{n} \frac{m_N^m m_E^a \Gamma(a_E+n) \gamma_{s,N}^{m-n} (2^{R_{s,N}} \gamma_E)^n e^{-\frac{m_N \gamma_{s,N}}{\gamma_0 \lambda_{NS}}}}{m! p! \Gamma(a_E) \lambda_{ES}^a \lambda_{NS}^m \gamma_0^m [B_{N,II}^{(2)}]^{a_E+n}}.$$

Proof: The proof of this theorem is similar to the proof of Theorem 2 in Appendix C, in which $F_{Y_{i,II}}(x)$ in (15) is used instead of $F_{Y_{i,I}}(x)$ in (11). ■

Based on (43) and (44), the overall SOP of the system in the case of Solution II is given by

$$SOP_{O,II} = 1 - (1 - SOP_{F,II})(1 - SOP_{N,II}). \quad (45)$$

2) *Asymptotic Secrecy Outage Probability Analysis:* Following the similar calculation steps as in IV-B2, with Solution II, the asymptotic SOP of user F is approximated as

$$SOP_{F,II}^{asym} \approx \sum_{m=0}^{a_E-1} \sum_{i=0}^N \Psi_{F,II}^{asym} h_{F,II}^{asym} \left[\frac{(v_i+1) u_F}{2} \right] + \sum_{m=0}^{a_E-1} \Psi_{F,E}, \quad (46)$$

$$\text{where } \Psi_{F,II}^{asym} = \frac{\pi u_F \alpha_F \sqrt{1-v_i^2}}{m! [(a_F)!]^{L_S} 2N} \left(\frac{m_F}{\gamma_0 \lambda_{FS}} \right)^{b_F} \left(\frac{m_E}{\gamma_E \lambda_{ES}} \right)^m,$$

$$h_{F,II}^{asym}(x) = \left(\frac{m_E A_x}{\gamma_E \lambda_{ES}} - m \right) \frac{A_{g_{x,F}}^{b_F} A_x^{m-1} e^{-\frac{m_E A_x}{\gamma_E \lambda_{ES}}}}{(\alpha_F - \alpha_N x)^2}, \quad \text{and } b_F = a_F L_S.$$

From (46), we conclude that secrecy diversity order at F in this case is $D_{F,II} = 0$.

Next, the asymptotic SOP at N is given by

$$SOP_{N,II}^{asym} = \begin{cases} 1, & \gamma_F \geq \beta \\ \Lambda_{1,II}^{asym} + \Lambda_{2,II}^{asym} + \Lambda_{3,II}^{asym}, & \gamma_F < \beta \end{cases}, \quad (47)$$

where

$$\Lambda_{1,II}^{asym} \approx \frac{1}{(a_N)!} \left(\frac{m_N A_{\gamma_F}}{\gamma_0 \lambda_{NS}} \right)^{a_N},$$

$$\Lambda_{2,II}^{asym} \approx \begin{cases} 0, & R_{s,N} < \eta \\ \frac{(m_N / \gamma_0 \lambda_{NS})^{a_N}}{(a_N)!} F_{Z_i} \left(\frac{A_{\gamma_F}}{\gamma_E} \right) \times (\gamma_{s,N}^{a_N} - A_{\gamma_F}^{a_N}), & R_{s,N} > \eta \end{cases},$$

$$\Lambda_{3,II}^{asym} \approx B_{N,II}^{asym} + \sum_{m=0}^{a_N} \sum_{n=0}^{a_E+m-1} \Psi_{N,II}^{asym} \left[\frac{m_E A_{\gamma_F}}{\gamma_E \lambda_{ES}} \right]^n e^{-\frac{m_E A_{\gamma_F}}{\gamma_E \lambda_{ES}}},$$

$$\text{with } B_{N,II}^{asym} = \frac{(m_N A_{\gamma_F} / \gamma_0 \lambda_{NS})^{a_N}}{(a_N)!} \left[F_{Z_i} \left(\frac{A_{\gamma_F}}{\gamma_E} \right) - 1 \right], \quad \text{and}$$

$$\Psi_{N,II}^{asym} = \binom{a_N}{m} \frac{m_N^a \Gamma(a_E+m) \gamma_{s,N}^{a_N-m} (2^{R_{s,N}} \gamma_E)^m \lambda_{ES}^m}{n! (a_N)! \Gamma(a_E) (\gamma_0 \lambda_{NS})^{a_N} m_E^m}.$$

It is shown from (47) that the secrecy diversity order at user N in the case of Solution II as

$$D_{N,II} = \begin{cases} 0, & \gamma_F \geq \beta \\ a_N, & \gamma_F < \beta \end{cases}. \quad (48)$$

From (46) and (47), the asymptotic overall SOP as

$$SOP_{O,II}^{asym} = 1 - \left(1 - SOP_{F,II}^{asym} \right) \left(1 - SOP_{N,II}^{asym} \right), \quad (49)$$

and the achieved overall secrecy diversity order in this case is $D_{O,II} = 0$.

Remark 4. *It is worth noting that Solution II provides the secrecy diversity order $m_N L_N$ (if $\gamma_F < \beta$) and 0 (if $\gamma_F \geq \beta$) for N . Thus, in this case, the secrecy performance of N does not depend on L_S . Also, it can be improved by increasing m_N and L_N . Solution II also brings the zero secrecy diversity order for both F and the overall system similar to Solution I.*

V. NUMERICAL RESULTS AND DISCUSSIONS

In this section, numerical results, in terms of the SOP, are provided to evaluate the secrecy performance of our solutions for designing the secure MIMO NOMA network.

Specifically, the SOP of F (i.e., SOP_F), N (i.e., SOP_N), and the overall system (i.e., SOP_O) are investigated in the cases of two different TAS solutions (i.e., Solutions I and II). Without loss of generality, it is assumed that the distance from S to F is set to unity and N is located between in them. Indeed, this setting has been widely used in the literature [28], [29]. In more details, the coordinates of S , F , N , and E are (0,0.5), (1,0.5), (0.5,0.5), and (3,0), respectively. Furthermore, the predetermined simulation parameters are set as follows: the target data rate and the secrecy rate thresholds $R_F = R_{s,F} = R_{s,N} = 0.5$ (bps/Hz), the path-loss exponents $\theta_{FS} = \theta_{NS} = \theta_{ES} = 2$, and the complexity-accuracy trade-off parameter $N = 100$.

In Figs. 2, 3, and 4, we examine SOP_N , SOP_F , and SOP_O as a function of average transmit SNR for LUs (γ_0) with different values of γ_E . It is observed that the secrecy performance evaluated at N , F and for the overall system are significantly improved (i.e., SOP_N , SOP_F , and SOP_O

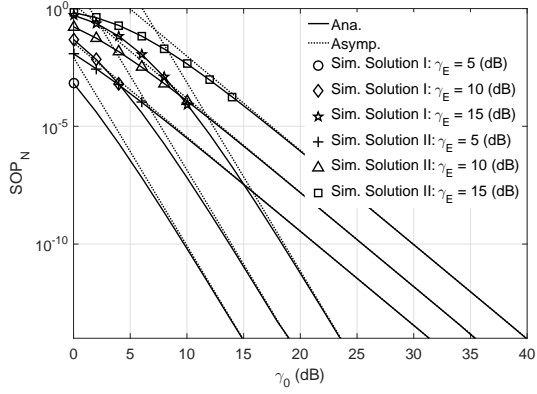


Fig. 2. SOP_N v.s. γ_0 with different values of γ_E , where $m_F = m_N = m_E = 2$, $L_S = L_N = L_E = 2$, $\alpha_F = 0.6$, and $\alpha_N = 0.4$.

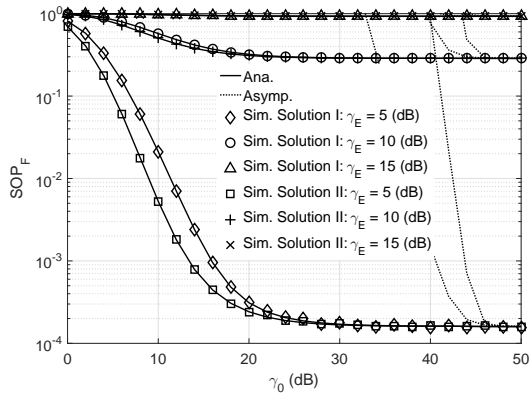


Fig. 3. SOP_F v.s. γ_0 with different values of γ_E , where $m_F = m_N = m_E = 2$, $L_S = L_F = L_E = 2$, $\alpha_F = 0.6$, and $\alpha_N = 0.4$.

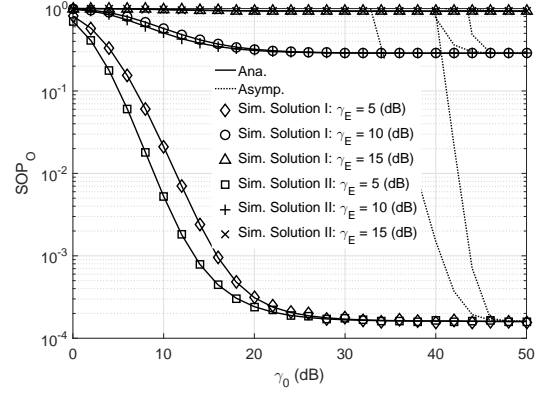


Fig. 4. SOP_O v.s. γ_0 with the different values of γ_E , where $m_F = m_N = m_E = 2$, $L_S = L_F = L_N = L_E = 2$, $\alpha_F = 0.6$, and $\alpha_N = 0.4$.

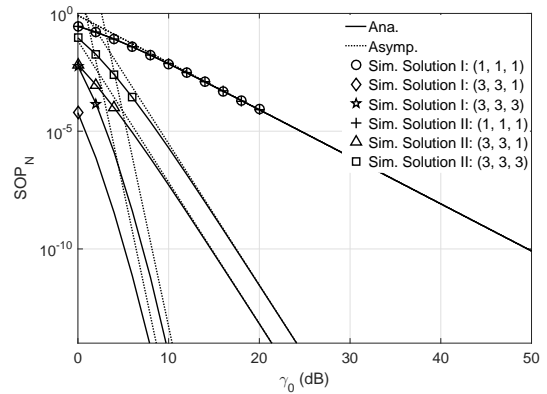


Fig. 5. SOP_N v.s. γ_0 with different values of (L_S, L_N, L_E) , where $m_F = m_N = m_E = 2$, $\alpha_F = 0.6$, $\alpha_N = 0.4$, and $\gamma_E = 10$ (dB).

decrease) when the higher values of γ_0 and the smaller values of γ_E are considered. Particularly, one can see that SOP_F and SOP_O remain constant in the high γ_0 regime, i.e., $\gamma_0 \rightarrow \infty$. In other words, the secrecy performance obtained at F and the secrecy performance of the overall system are saturated. Then, this phenomenon confirms the calculation of the zero secrecy diversity order for F and the overall system in both Solution I and Solution II, as indicated in IV-B2 and IV-C2.

In order to study how using multiple antennas impacts on the secrecy performance, we investigate the variations of SOP_N , SOP_F , and SOP_O with respect to the different values of the number of antennas at S , F , N , and E , denoted by (L_S, L_F, L_N, L_E) , as illustrated in Figs. 5, 6, and 7, respectively. Particularly, in the case of $(L_S, L_F, L_N, L_E) = (1, 1, 1, 1)$, Solutions I and II yield the same curves. In general, it is visible that employing MIMO at the LUs improves the secrecy performance significantly. In addition, the more antennas the eavesdropper has, the worse security performance the system is. More specific discussions regarding these figures are following.

As observed in Fig. 5, the decrease in L_E and the increase in L_N and L_S bring the positive effects on the secrecy performance evaluated at N . Furthermore, as shown in IV-B2 and IV-C2, the secrecy diversity order at N are $m_N L_N L_S$ and

$m_N L_N$ in the cases of Solution I and Solution II ($\gamma_F < \beta$), respectively. In other words, considering Solution I, a profound improvement of the secrecy performance can be obtained by increasing m_N , L_N , and L_S . However, accounting for Solution II, the improvement can only occur with the higher values of m_N and L_N .

In Fig. 6, SOP_F decreases when L_F and L_S increase as well as L_E decreases. However, as above-mentioned, in the high γ_0 regime, the secrecy performance at F achieves the saturation which does not depend on the number of antennas (i.e., L_F and L_S). The similar phenomenon can also be observed when considering the effect of (L_S, L_F, L_N, L_E) on SOP_O in Fig. 7. Specifically, the overall secrecy performance can be improved as L_S , L_F , and L_N scale up or L_E scales down in the low and medium range of γ_0 . Moreover, in the high γ_0 regime, L_S , L_F , and L_N have no impact on SOP_O and then the overall system reaches a secrecy performance floor.

In the NOMA system, the secrecy performance depends on the power allocation coefficients, i.e., α_F and α_N . Therefore, Fig. 8 is provided to clarify the effect of α_F and α_N on the secrecy performance of the overall system, where $\alpha_F > \alpha_N > 0$ and $\alpha_N = 1 - \alpha_F$. From this figure, one can see that there is a pair of optimal values of α_F and α_N that maximize the overall

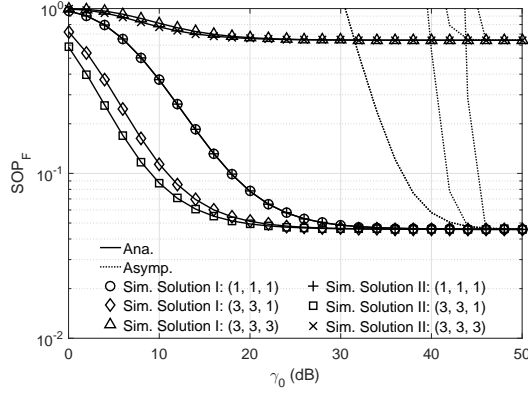


Fig. 6. SOP_F v.s. γ_0 with different values of (L_S, L_F, L_E) , where $m_F = m_N = m_E = 2$, $\alpha_F = 0.6$, $\alpha_N = 0.4$, and $\gamma_E = 10$ (dB).

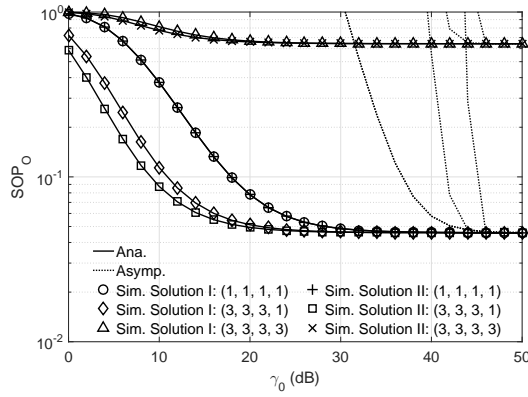


Fig. 7. SOP_O v.s. γ_0 with the different values of (L_S, L_F, L_N, L_E) , where $m_F = m_N = m_E = 2$, $\alpha_F = 0.6$, $\alpha_N = 0.4$, and $\gamma_E = 10$ (dB).

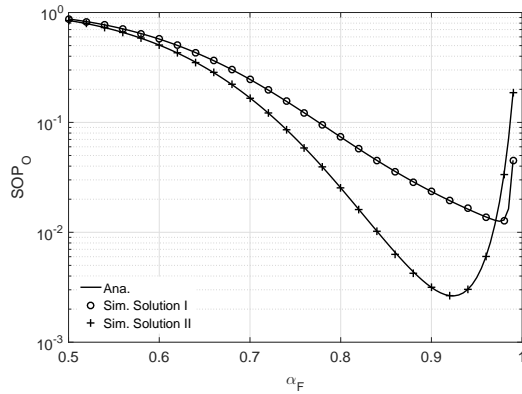


Fig. 8. SOP_O v.s. α_F , where $m_F = m_N = m_E = 2$, $L_S = L_F = L_N = L_E = 2$ and $\gamma_0 = \gamma_E = 10$ (dB).

secrecy performance. Thus, α_F and α_N should be properly selected to enhance the secrecy performance of the overall system.

In Fig. 9, the effect of fading parameters, i.e., m_N , m_F , and m_E , on the overall secrecy performance is investigated. In this case, Nakagami- m distribution is used to show more general insights regarding channel models. Specifically, Nakagami- m

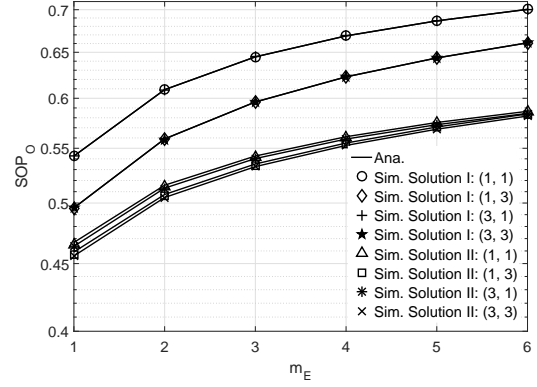


Fig. 9. SOP_O v.s. m_E with different values of (m_N, m_F) , where $\alpha_F = 0.6$, $\alpha_N = 0.4$, $L_S = L_F = L_N = L_E = 2$, and $\gamma_0 = \gamma_E = 10$ (dB).

fading corresponds to Rayleigh fading as $m = 1$, whereas it approximates Rician fading with parameter K as $m = (K + 1)^2 / (2K + 1)$. We can see from this figure that the improvement of the secrecy performance is observed with the increases in m_N and m_F and the decrease in m_E . This can be explained by that the better legitimate channel quality and the worse illegitimate channel quality are obtained when increasing m_N and m_F and decreasing m_E , respectively. In addition, Fig. 9 indicates that m_F has a stronger impact on the overall secrecy performance than m_N does.

In order to clarify the effectiveness of our proposed protocol, the comparison between our protocol and conventional ones given in [21]–[23], denoted by SOP_O , is presented in Fig. 10. Furthermore, the results regarding the WcES are provided in the figure as a benchmark. It can be observed from Fig. 10 that in our proposed protocol, the WcES yields a significant decrease in the secrecy performance. This is because the eavesdropper has the ability of powerfully detecting multi-user data without the interference in this case. Comparing with the previous works [21]–[23], we obtain the following different results:

- Our protocol gives a much better overall secrecy performance, compared with the protocol in [21]. It can be explained by the fact that the solution in [21] overestimates the eavesdropper's multi-user decodability, which may be a non-trivial task, and hence leads to the significant reduction of the secrecy performance.
- Fig. 10 shows that nothing of significance has changed in the secrecy performance obtained from our protocol and the method in [22]. However, our protocol brings more practical and general insights. In fact, the assumption used in [21], [22] (i.e., the strong user always successfully decodes the message of the weak user) is a strong one and may be difficult to achieve in realistic scenarios.
- Our protocol achieves better secrecy performance than the protocol in [23] since the solution in [23] still considered WcES. Note that our protocol can achieve the results similar to the solution in [23] in case of the WcES.

It is noteworthy from all results that the secrecy performance at N is much better than that at F (i.e., SOP_N is much less

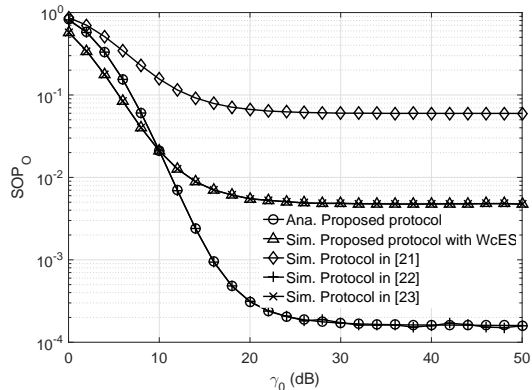


Fig. 10. Comparison of secure communication protocols with Solution I, where $m_F = m_N = m_E = 2$, $\alpha_F = 0.6$, $\alpha_N = 0.4$, $\gamma_E = 5$ (dB), $L_S = L_F = L_N = 2$, and $L_E = 1$.

than SOP_F). It can be explained by the fact that $S \rightarrow N$ link has a better channel gain than $S \rightarrow F$ link does since N is closer to S than F does. In addition, one can see that Solution I brings a better secrecy performance for N over Solution II, whereas Solution II offers a higher secrecy performance for F than Solution I does. This can be explained according to the principle of TAS solutions presented in section III. Taking the overall secrecy performance into account, it can be evaluated that Solution II outperforms Solution I. This implies guaranteeing the secure performance at F has a stronger impact on the overall secrecy performance than that at N .

VI. CONCLUSION

In this work, we considered a two-user MIMO NOMA network in the presence of an eavesdropper over Nakagami- m channels. Accordingly, we proposed two TAS solutions to design the secure communication protocol for the network. To validate the solutions, we evaluated the secrecy performance of the system by deriving the exact and asymptotic closed-form expressions of the SOP at the LUs and the SOP of the overall system. Numerical results demonstrated that increasing the number of antennas at the source and the LUs enhances the overall secrecy performance in the low and medium ranges of the average transmit SNR values (γ_0), however, this has no impact on the performance when $\gamma_0 \rightarrow \infty$. In addition, properly choosing α_F and α_N can yield a better overall secrecy performance. Furthermore, our proposed protocol brings not only an improved secrecy performance but also more practical and general insights, compared with previous protocols. Interestingly, Solution II outperforms Solution I regarding the secrecy performance even when they achieve the same zero overall secrecy diversity order.

APPENDIX A

PROOF OF EQUATION (28)

We rewrite Θ_1 , Θ_2 , and Θ_3 in (28) as follows:

$$\begin{aligned} \Theta_1 &= \Pr \{ (\alpha_F - \alpha_N \gamma_F) \gamma_0 Y_i < \gamma_F \} \\ &= \begin{cases} 1, & \gamma_F \geq \beta \\ F_{Y_i} \left(\frac{A_{\gamma_F}}{\gamma_0} \right) = \Lambda_1, & \gamma_F < \beta \end{cases}, \end{aligned} \quad (50)$$

$$\begin{aligned} \Theta_2 &= \Pr \{ (\alpha_F - \alpha_N \gamma_F) \gamma_0 Y_i \geq \gamma_F, \\ &\quad (\alpha_F - \alpha_N \gamma_F) \gamma_E Z_i < \gamma_F, Y_i < \gamma_{s,N} / \gamma_0 \} \\ &= \begin{cases} 0, & \gamma_F \geq \beta \\ \underbrace{\Pr \left\{ Y_i \geq \frac{A_{\gamma_F}}{\gamma_0}, Z_i < \frac{A_{\gamma_F}}{\gamma_E}, Y_i < \frac{\gamma_{s,N}}{\gamma_0} \right\}}_{\Lambda_2}, & \gamma_F < \beta \end{cases}, \end{aligned} \quad (51)$$

and

$$\Theta_3 = \begin{cases} 0, & \gamma_F \geq \beta \\ \underbrace{\Pr \left\{ Y_i \geq \frac{A_{\gamma_F}}{\gamma_0}, Z_i \geq \frac{A_{\gamma_F}}{\gamma_E}, \right. \\ \left. Y_i < \frac{2^{R_{s,N}} \gamma_E Z_i + \gamma_{s,N}}{\gamma_0} \right\}}_{\Lambda_3}, & \gamma_F < \beta \end{cases}. \quad (52)$$

To calculate Λ_2 , we observe that if $\frac{A_{\gamma_F}}{\gamma_0} > \frac{\gamma_{s,N}}{\gamma_0}$ or $R_{s,N} < \eta$ then $\Lambda_2 = 0$, otherwise, $\Lambda_2 = \Pr \left\{ \frac{A_{\gamma_F}}{\gamma_0} \leq Y_i < \frac{\gamma_{s,N}}{\gamma_0}, Z_i < \frac{A_{\gamma_F}}{\gamma_E} \right\}$. By using the definition of the CDF, Λ_2 is expressed as

$$\Lambda_2 = \begin{cases} 0, & R_{s,N} < \eta \\ \left[F_{Y_i} \left(\frac{\gamma_{s,N}}{\gamma_0} \right) - F_{Y_i} \left(\frac{A_{\gamma_F}}{\gamma_0} \right) \right] \\ \times F_{Z_i} \left(\frac{A_{\gamma_F}}{\gamma_E} \right), & R_{s,N} > \eta \end{cases}, \quad (53)$$

Regarding Λ_3 , we observe that if $\frac{2^{R_{s,N}} \gamma_E Z_i + \gamma_{s,N}}{\gamma_0} < \frac{A_{\gamma_F}}{\gamma_0}$ or $Z_i < \frac{A_{\gamma_F} - \gamma_{s,N}}{2^{R_{s,N}} \gamma_E}$ then $\Lambda_3 = 0$, otherwise, $\Lambda_3 = \Pr \left\{ \frac{A_{\gamma_F}}{\gamma_0} \leq Y_i < \frac{2^{R_{s,N}} \gamma_E Z_i + \gamma_{s,N}}{\gamma_0}, Z_i \geq \frac{A_{\gamma_F}}{\gamma_E} \right\}$. Since $\frac{A_{\gamma_F} - \gamma_{s,N}}{2^{R_{s,N}} \gamma_E} < \frac{A_{\gamma_F}}{\gamma_E}$, $\forall \gamma_F < \beta$, hence Λ_3 is given by

$$\begin{aligned} \Lambda_3 &= \int_{\frac{A_{\gamma_F}}{\gamma_E}}^{\infty} \int_{\frac{A_{\gamma_F}}{\gamma_0}}^{\frac{2^{R_{s,N}} \gamma_E Z_i + \gamma_{s,N}}{\gamma_0}} f_{Y_i}(y) f_{Z_i}(x) dy dx \\ &= \int_{\frac{A_{\gamma_F}}{\gamma_E}}^{\infty} \left[F_{Y_i} \left(\frac{2^{R_{s,N}} \gamma_E x + \gamma_{s,N}}{\gamma_0} \right) - F_{Y_i} \left(\frac{A_{\gamma_F}}{\gamma_0} \right) \right] \\ &\quad \times f_{Z_i}(x) dx. \end{aligned} \quad (54)$$

From (50) to (54), $SOP_{N,i}$ is obtained as in (28) and the proof is completed.

APPENDIX B

PROOF OF THEOREM 1

By using Lemma 1, $F_{\gamma_{FS_i}^{x_F}, I}(g_{x,F})$ is expressed as

$$\begin{aligned} &F_{\gamma_{FS_i}^{x_F}, I}(g_{x,F}) \\ &= \begin{cases} 1, & x \geq u_F \\ 1 - \sum_{k=0}^{a_F-1} \frac{1}{k! \lambda_{FS}^k} \left(\frac{m_F A_{g_{x,F}}}{\gamma_0} \right)^k e^{-\frac{m_F A_{g_{x,F}}}{\gamma_0 \lambda_{FS}}}, & x < u_F \end{cases}. \end{aligned} \quad (55)$$

Based on Lemma 3 and (55), SOP of user F in (29) can be rewritten as

$$\begin{aligned} SOP_{F,I} &= \sum_{k=0}^{a_E-1} \frac{m_E^k \alpha_F}{k! \lambda_{ES}^k \gamma_E^k} \int_0^\beta \frac{A_x^{k-1} e^{-\frac{m_E A_x}{\gamma_E \lambda_{ES}}}}{(\alpha_F - \alpha_N x)^2} \left(\frac{m_E A_x}{\lambda_{ES} \gamma_E} - k \right) dx \\ &\quad - \sum_{m=0}^{a_F-1} \sum_{n=0}^{a_E-1} \frac{\alpha_F m_F^m m_E^n}{m! n! \lambda_{FS}^m \lambda_{ES}^n \gamma_0^m \gamma_E^n} \int_0^{u_F} h_{F,I}(x) dx \\ &= 1 - \sum_{m=0}^{a_F-1} \sum_{n=0}^{a_E-1} \frac{\alpha_F m_F^m m_E^n}{m! n! \lambda_{FS}^m \lambda_{ES}^n \gamma_0^m \gamma_E^n} \int_0^{u_F} h_{F,I}(x) dx, \end{aligned} \quad (56)$$

where, (56) is obtained by the fact that $u_F \leq \beta$, $\forall R_{s,F} \geq 0$ and $h_{F,I}(x) = \frac{A_{g_{x,F}}^m A_x^{n-1}}{(\alpha_F - \alpha_N x)^2} e^{-\frac{m_F A_{g_{x,F}}}{\gamma_0 \lambda_{FS}} - \frac{m_E A_x}{\gamma_E \lambda_{ES}}} \left(\frac{m_E A_x}{\gamma_E \lambda_{ES}} - n \right)$. Note that it is challenging to resolve the integral in (56), hence an approximation solution is proposed by using the Gaussian-Chebyshev quadrature [30] as follows:

$$\int_0^{u_F} h_{F,I}(x) dx \approx \frac{\pi u_F}{2N} \sum_{i=0}^N h_{F,I} \left[\frac{(v_i + 1) u_F}{2} \right] \sqrt{1 - v_i^2}. \quad (57)$$

By substituting (57) into (56), $SOP_{F,I}$ is obtained as in (31). The proof of Theorem 1 is completed.

APPENDIX C PROOF OF THEOREM 2

From (28), SOP of user N in Solution I is expressed as in (32), in which $\Lambda_{1,I}$ and $\Lambda_{2,I}$ is obtained by substituting $F_{Y_{i,I}}(x)$ in (11) and $F_{Z_{i,I}}(x)$ in (17) into Λ_1 and Λ_2 in (28). To derive $\Lambda_{3,I}$, we rewrite $\Lambda_{3,I}$ by substituting $F_{Y_{i,I}}(x)$ in (11) and $f_{Z_{i,I}}(x)$ in (16) into Λ_3 in (28) as follows:

$$\begin{aligned} \Lambda_{3,I} &= \underbrace{\left[1 - F_{Y_{i,I}} \left(\frac{A_{\gamma_F}}{\gamma_0} \right) \right]}_{B_{N,I}^{(1)}} \left[1 - F_{Z_{i,I}} \left(\frac{A_{\gamma_F}}{\gamma_E} \right) \right] \\ &\quad + \sum_{p=1}^{L_S} \sum_{\Delta_N=p} \frac{\Phi_N m_E^{a_E}}{\Gamma(m_E L_E) \lambda_{ES}^{a_E}} \int_{\frac{A_{\gamma_F}}{\gamma_E}}^{\infty} \left(\frac{2^{R_{s,N}} \gamma_E x + \gamma_{s,N}}{\gamma_0} \right)^{\varphi_N} \\ &\quad \times x^{a_E-1} e^{-\frac{pm_N (2^{R_{s,N}} \gamma_E x + \gamma_{s,N})}{\gamma_0 \lambda_{NS}} - \frac{m_E x}{\lambda_{ES}}} dx. \end{aligned} \quad (58)$$

By applying binomial expansion for $(2^{R_{s,N}} \gamma_E x + \gamma_{s,N})^{\varphi_N}$ and upper incomplete Gamma function [27, Eq. 8.350.2] into (58), $\Lambda_{3,I}$ is obtained as in (32). The proof of Theorem II is completed.

REFERENCES

- [1] Y. Saito, Y. Kishiyama, A. Benjebbour, T. Nakamura, and K. H. A. Li, "Non-orthogonal multiple access (NOMA) for cellular future radio access," in *Proc. Veh. Technol. Conf. (VTC Spring)*, Dresden, Germany, June 2013, pp. 1–5.
- [2] L. Dai, B. Wang, Y. Yuan, S. Han, C.-L. I, and Z. Wang, "Non-orthogonal multiple access for 5G: Solutions, challenges, opportunities, and future research trends," *IEEE Commun. Mag.*, vol. 53, no. 9, pp. 74–81, Sept. 2015.
- [3] Y. Liu, Z. Ding, M. Elkashlan, and H. V. Poor, "Cooperative non-orthogonal multiple access with simultaneous wireless information and power transfer," *IEEE J. Sel. Areas Commun.*, vol. 34, no. 4, pp. 938–953, Apr. 2016.

- [4] Z. Ding, Z. Yang, P. Fan, and H. V. Poor, "On the performance of non-orthogonal multiple access in 5G systems with randomly deployed users," *IEEE Signal Process. Lett.*, vol. 21, no. 12, pp. 1501–1505, Dec. 2014.
- [5] Z. Ding, M. Peng, and H. V. Poor, "Cooperative non-orthogonal multiple access in 5G systems," *IEEE Commun. Lett.*, vol. 19, no. 8, pp. 1462–1465, Aug. 2015.
- [6] D.-D. Tran, H.-V. Tran, D.-B. Ha, and G. Kaddoum, "Cooperation in noma networks under limited user-to-user communications: Solution and analysis," in *Proc. IEEE Wireless Commun. and Netw. Conf. (WCNC)*, Barcelona, Spain, April 2018, pp. 1–6.
- [7] A. D. Wyner, "The wire-tap channel," *Bell Syst. Tech. J.*, vol. 54, no. 8, pp. 1355–1387, Oct. 1975.
- [8] I. Csiszár and J. Körner, "Broadcast channels with confidential messages," *IEEE Trans. Inf. Theory*, vol. 24, no. 3, pp. 339–348, May 1978.
- [9] M. Bloch, J. Barros, M. R. Rodrigues, and S. W. McLaughlin, "Wireless information-theoretic security," *IEEE Trans. Inf. Theory*, vol. 54, no. 6, pp. 2515–2534, June 2008.
- [10] S. Bashar, Z. Ding, and G. Y. Li, "On secrecy of codebook-based transmission beamforming under receiver limited feedback," *IEEE Trans. Wireless Commun.*, vol. 10, no. 4, pp. 1212–1223, Apr. 2011.
- [11] D.-D. Tran, N. S. Vo, T. L. Vo, and D.-B. Ha, "Physical layer secrecy performance of multi-hop decode-and-forward relay networks with multiple eavesdroppers," in *Proc. Int. Conf. on Adv. Inf. Netw. and Appl. Workshops (WAINA)*, Gwangju, South Korea, Mar. 2015.
- [12] D.-D. Tran, D.-B. Ha, V. T. Ha, and E.-K. Hong, "Secrecy analysis with MRC/SC-based eavesdropper over heterogeneous channels," *IETE J. of Research*, vol. 61, no. 4, pp. 363–371, Mar. 2015.
- [13] C. E. Shannon, "Communication theory of secrecy systems," *Bell Syst. Tech. J.*, vol. 28, pp. 656–715, Oct. 1949.
- [14] N. Yang, P. L. Yeoh, M. Elkashlan, R. Schober, and I. B. Collings, "Transmit antenna selection for security enhancement in MIMO wiretap channels," *IEEE Trans. Commun.*, vol. 61, no. 1, pp. 144–154, Jan. 2013.
- [15] L. Wang, M. Elkashlan, J. Huang, R. Schober, and R. Mallik, "Secure transmission with antenna selection in MIMO Nakagami- m fading channels," *IEEE Trans. Wireless Commun.*, vol. 13, no. 11, pp. 6054–6067, Nov. 2014.
- [16] S. Goel and R. Negi, "Guaranteeing secrecy using artificial noise," *IEEE Trans. Wireless Commun.*, vol. 7, no. 6, pp. 2180–2189, June 2008.
- [17] V. N. Vo, T. G. Nguyen, C. So-In, and D.-B. Ha, "Secrecy performance analysis of energy harvesting wireless sensor networks with a friendly jammer," *IEEE Access*, vol. 5, pp. 25 196–25 206, Oct. 2017.
- [18] A. Mukherjee and A. L. Swindlehurst, "Robust beamforming for security in MIMO wiretap channels with imperfect CSI," *IEEE Trans. Signal Process.*, vol. 59, no. 1, pp. 351–361, Jan. 2011.
- [19] Y. Zhang, H. M. Wang, Q. Yang, and Z. Ding, "Secrecy sum rate maximization in non-orthogonal multiple access," *IEEE Commun. Lett.*, vol. 20, no. 5, pp. 930–933, May 2016.
- [20] Z. Qin, Y. Liu, Z. Ding, Y. Gao, and M. Elkashlan, "Physical layer security for 5G non-orthogonal multiple access in large-scale networks," in *Proc. IEEE Int. Conf. Commun. (ICC)*, Kuala Lumpur, Malaysia, May 2016.
- [21] Y. Liu, Z. Qiu, M. Elkashlan, Y. Gao, and L. Hanzo, "Enhancing the physical layer security of non-orthogonal multiple access in large-scale networks," *IEEE Trans. Wireless Commun.*, vol. 16, no. 3, pp. 1656–1672, Mar. 2017.
- [22] H. Lei, J. Zhang, K. H. Park, P. Xu, I. S. Ansari, G. Pan, B. Alomair, and M. S. Alouini, "On secure NOMA systems with transmit antenna selection schemes," *IEEE Access*, vol. 5, pp. 17 450–17 464, Aug. 2017.
- [23] L. Lv, Z. Ding, Q. Ni, and J. Chen, "Secure MISO-NOMA transmission with artificial noise," *IEEE Trans. Veh. Technol.*, vol. 67, no. 7, pp. 6700–6705, July 2018.
- [24] G. Chen, J. P. Coon, and M. D. Renzo, "Secrecy outage analysis for downlink transmissions in the presence of randomly located eavesdroppers," *IEEE Trans. Inf. Forensics Security*, vol. 12, no. 5, pp. 1195–1206, May 2017.
- [25] Z. Ding, P. Fan, and H. V. Poor, "Impact of user pairing on 5G non-orthogonal multiple access downlink transmission," *IEEE Trans. Veh. Technol.*, vol. 65, no. 8, pp. 6010–6023, Aug. 2016.
- [26] Z. Ding, F. Adachi, and H. V. Poor, "The application of MIMO to non-orthogonal multiple access," *IEEE Trans. Wireless Commun.*, vol. 15, no. 1, pp. 537–552, Jan. 2016.
- [27] I. Gradshteyn and I. Ryzhik, *Table of Integrals, Series, and Products*, 7th ed. Academic Press, Mar. 2007.
- [28] H. Chen, Y. Li, J. L. Rebelatto, B. F. Ucha-Filho, and B. Vucetic, "Harvest-then-cooperate: Wireless-powered cooperative communica-

- tions," *IEEE Trans. Signal Process.*, vol. 63, no. 7, pp. 1700–1711, Apr. 2015.
- [29] L. Fan, N. Yang, T. Q. Duong, M. ElKashlan, and G. K. Karagiannidis, "Exploiting direct links for physical layer security in multiuser multirelay networks," *IEEE Trans. Wireless Commun.*, vol. 15, no. 6, pp. 3856–3867, June 2016.
- [30] F. B. Hildebrand, *Introduction to numerical analysis*. New York, USA: Dover Publications, 1987.